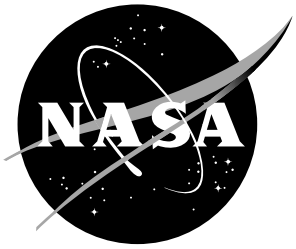
NASA/TM–2019-220430



Over-the-Rotor Liner Investigation via the NASA Langley Normal Incidence Tube

Michael G. Jones, Martha C. Brown, and Brian M. Howerton
Langley Research Center, Hampton, Virginia

Lawrence E. Becker
Analytical Services & Materials, Hampton, Virginia

November 2019

NASA STI Program. . . in Profile

Since its founding, NASA has been dedicated to the advancement of aeronautics and space science. The NASA scientific and technical information (STI) program plays a key part in helping NASA maintain this important role.

The NASA STI Program operates under the auspices of the Agency Chief Information Officer. It collects, organizes, provides for archiving, and disseminates NASA's STI. The NASA STI Program provides access to the NASA Aeronautics and Space Database and its public interface, the NASA Technical Report Server, thus providing one of the largest collection of aeronautical and space science STI in the world. Results are published in both non-NASA channels and by NASA in the NASA STI Report Series, which includes the following report types:

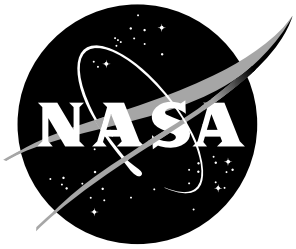
- TECHNICAL PUBLICATION. Reports of completed research or a major significant phase of research that present the results of NASA programs and include extensive data or theoretical analysis. Includes compilations of significant scientific and technical data and information deemed to be of continuing reference value. NASA counterpart of peer-reviewed formal professional papers, but having less stringent limitations on manuscript length and extent of graphic presentations.
- TECHNICAL MEMORANDUM. Scientific and technical findings that are preliminary or of specialized interest, e.g., quick release reports, working papers, and bibliographies that contain minimal annotation. Does not contain extensive analysis.
- CONTRACTOR REPORT. Scientific and technical findings by NASA-sponsored contractors and grantees.
- CONFERENCE PUBLICATION. Collected papers from scientific and technical conferences, symposia, seminars, or other meetings sponsored or co-sponsored by NASA.
- SPECIAL PUBLICATION. Scientific, technical, or historical information from NASA programs, projects, and missions, often concerned with subjects having substantial public interest.
- TECHNICAL TRANSLATION. English-language translations of foreign scientific and technical material pertinent to NASA's mission.

Specialized services also include organizing and publishing research results, distributing specialized research announcements and feeds, providing information desk and personal search support, and enabling data exchange services.

For more information about the NASA STI Program, see the following:

- Access the NASA STI program home page at `http://www.sti.nasa.gov`
- E-mail your question to `help@sti.nasa.gov`
- Phone the NASA STI Information Desk at 757-864-9658
- Write to:
  NASA STI Information Desk
  Mail Stop 148
  NASA Langley Research Center
  Hampton, VA 23681-2199

NASA/TM–2019–220430



Over-the-Rotor Liner Investigation via the NASA Langley Normal Incidence Tube

Michael G. Jones, Martha C. Brown, and Brian M. Howerton
Langley Research Center, Hampton, Virginia

Lawrence E. Becker
Analytical Services & Materials, Hampton, Virginia

National Aeronautics and
Space Administration

Langley Research Center
Hampton, Virginia 23681-2199

November 2019

Acknowledgments

This work was funded by the Advanced Air Transport Technology Project of the NASA Advanced Air Vehicles Program.

The use of trademarks or names of manufacturers in this report is for accurate reporting and does not constitute an offical endorsement, either expressed or implied, of such products or manufacturers by the National Aeronautics and Space Administration.

Available from:

NASA STI Program / Mail Stop 148
NASA Langley Research Center
Hampton, VA 23681-2199
Fax: 757-864-6500

Abstract

NASA Langley and Glenn Research Centers have collaborated on the usage of acoustic liners mounted very near or directly over the rotor of turbofan aircraft engines. This collaboration began over a decade ago with the investigation of a metallic foam liner. Similar to conventional acoustic liner applications, this liner was designed to absorb sound generated by the rotor-alone and rotor-stator interaction sources within the fan duct. Given its proximity to the rotor tips, the expectation was that the liner would also serve as a pressure release and thereby inhibit the amount of noise generated. Initial acoustic results were promising, but there was concern regarding potential aerodynamic penalties. Nevertheless, there were sufficient positive results to warrant further investigation. To that end, the current report presents results obtained in the NASA Langley Normal Incidence Tube for 20 acoustic liner candidates for the OTR application. The majority contain grooves at their surface, designed to minimize aerodynamic penalties caused by placing the liner in close proximity to the fan rotor tips. The intent is to assess the acoustic properties of each liner configuration, and in particular to assess the effects of including the grooves on the overall acoustic performance. An additional intent of this paper is to provide documentation regarding recent enhancements to the NASA Langley Normal Incidence Tube.

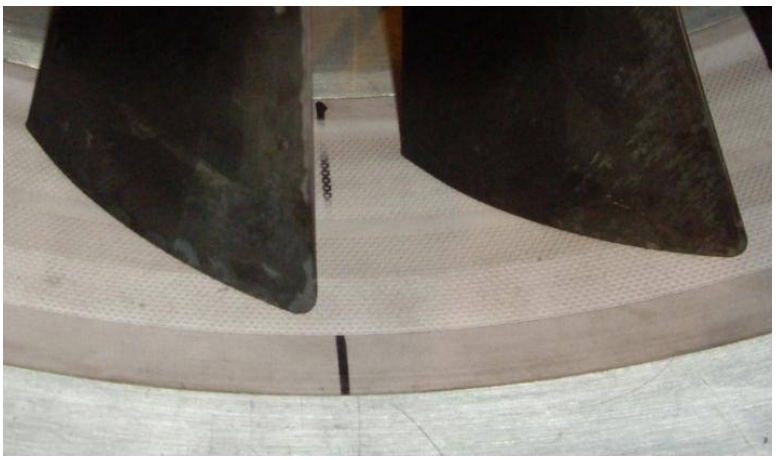
1 Introduction

Passive acoustic liners are a key contributor in the reduction of fan noise propagated through the inlet and aft-fan duct of aircraft engine nacelles. These liners are typically mounted in the walls of the inlet and in the inner and outer walls of the aft bypass duct, and are generally intended to absorb sound that has been generated by the rotor (rotor-alone noise) or by rotor-stator interactions. The NASA Langley Normal Incidence Tube (NIT) has been used for initial evaluation of numerous conventional and novel liner concepts for over four decades. One of the novel acoustic liner applications of recent interest at NASA is the over-the-rotor (OTR) liner [1–10]. As the name suggests, these are acoustic liners mounted either directly over or very near to the rotor. These liners provide a pressure release surface very near the source such that the source strength is reduced, and also absorb some of the remaining sound that is generated, similar to the liners mounted in the inlet and aft-bypass duct.

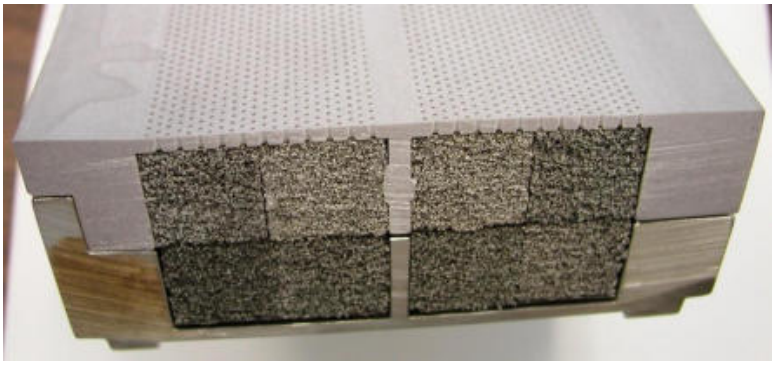
One of the first OTR concepts (see Fig. 1) employed a single-degree-of-freedom (SDOF) liner for which the core chambers were filled with metallic foam to achieve a desired impedance spectrum at the surface of the liner. A number of tests were conducted at both NASA Langley and Glenn Research Centers to cover a range of Technology Readiness Levels.[1] The metallic foams considered for this application provided excellent fan containment properties, and also provided very good acoustic

[1]Technology Readiness Level (TRL) is a term used by NASA to indicate the maturity of a particular concept. A TRL of 1 is assigned to a basic concept that has not yet been developed, whereas a TRL of 9 is applied to a concept that has been fully matured and is used in flight.

results in component tests with the Langely Normal Incidence Tube (NIT), low TRL tests in the Glenn Advanced Noise Control Fan (ANCF), and engine tests with an FJ44 engine [4]. However, tests with this concept had to be aborted in the GRC 22-in Fan Rig due to problems with increased air jetting and/or metal foam impingement onto the blade surface. Also, the performance penalty was observed to vary widely. Some of the acoustic variability was determined to be due to fabrication and installation procedures, while the performance penalty appeared to be largely driven by the geometry (or presence) of grooves at the surface of the liner. Nevertheless, the successful results of the lower TRL tests (and the FJ44 engine test) suggested the initial choice of surface impedance was appropriate for this application, but more detailed analysis was needed to more thoroughly explore the OTR application.



(a) Perforate rubstrip over metal foam.



(b) Edge view of metal foam installed beneath perforate.

Figure 1: Photographs of over-the-rotor metallic foam liner with perforate rubstrip.

The primary purpose of the current report is to explore results achieved in the inital portion of this follow-on study, which was conducted using the NASA Langley Normal Incidence Tube (NIT, see Fig. 2). For this study, a large number of acoustic

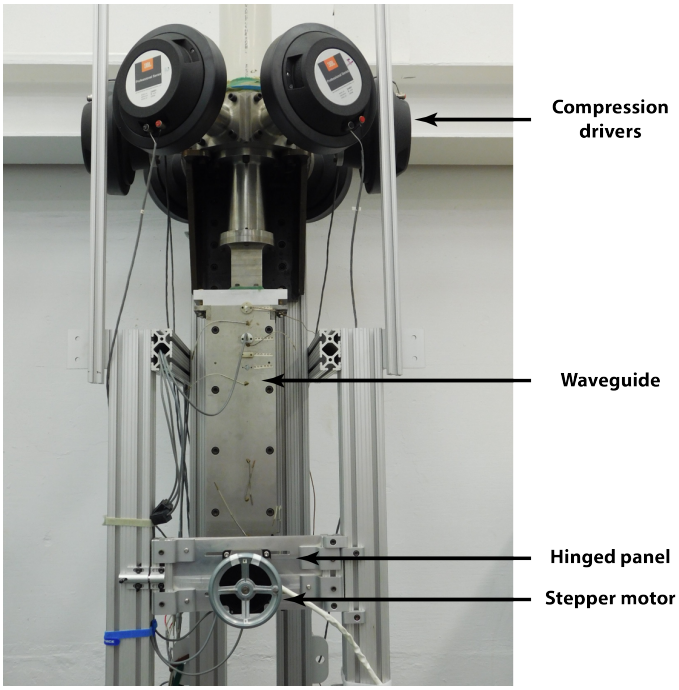


Figure 2: Photograph of NASA Langley Normal Incidence Tube (NIT).

liner configurations were considered for use in the OTR application. These configurations included the SDOF with metallic foam configuration, but also included a number of other liner concepts. For all but a few baseline hardwall configurations, these liner configurations contain grooves at their surface. The intent was to assess the acoustic properties of each liner configuration, and in particular to assess the effects of including the grooves on the overall acoustic performance. These results were subsequently used to select liner configurations for further study in the NASA Langley grazing flow impedance tube (GFIT) and the NASA Glenn W-8 Wind Tunnel [9].

Section 2 presents a description of the NIT and the test samples, and Section 3 provides the corresponding results. Some of the more important results are listed in the Concluding Remarks. Over the past few years, a number of NIT enhancements have been implemented to enable more efficient evaluation of liner concepts. A secondary purpose of this report is therefore to provide an overview of the current NIT operation. This overview is provided in Appendix 4.

2 Experimental Method

Normal Incidence Tube

The NASA Langley Normal Incidence Tube (NIT, see Figs. 2 and 3) is a zero-flow, vertical-standing test apparatus designed to measure the acoustic impedance of air-

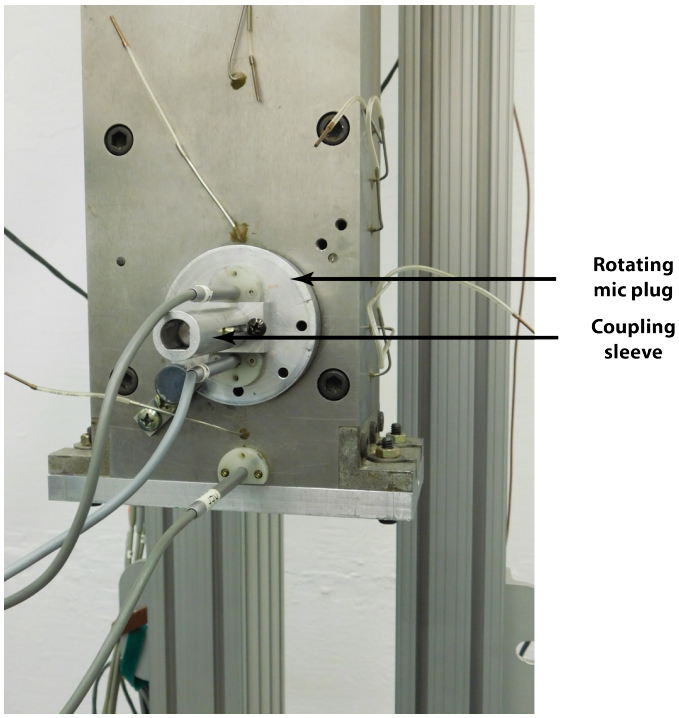


Figure 3: Close-up view of NIT rotating microphone plug.

craft liner samples. Via the Two-Microphone Method [11, 12], the normal-incidence impedance of materials can be determined by the generation of plane waves from six 120-W compression drivers at the upper end of a 2-in×2-in waveguide tube, and the measurement of noise spectral levels above a test specimen mounted approximately three-feet below the drivers. A rotating plug containing two microphones provides a mechanism for the systematic collection of complex acoustic pressures. Specifically, the transfer function is measured between microphones at two prescribed distances (2.5 and 3.75 in) from the liner surface such that the frequency dependence of the no-flow acoustic impedance of the liner can be computed.

The current study is conducted using two source types: tonal and random. Tonal tests (one frequency at a time) are conducted for source frequencies of 400 to 3000 Hz in 200 Hz increments, with target source sound pressure levels (SPLs) of 120, 140 and 150 dB at the reference microphone. These tones are digitally synthesized and converted to analog waveforms for input to the acoustic drivers. The random noise source (often labeled as broadband) consists of Gaussian white noise generated by a random noise generator. For this source, the partial overall sound pressure level (integrated from 400 to 3000 Hz) at the reference microphone is set to a target level, and the acoustic pressure data are processed in 12.5 Hz increments. Whereas the tonal source allows the precise study of the effects of frequency on the resultant impedance, the random source provides understanding regarding the interactive ef-

fects of different frequencies on the liner impedance. For both sources, multiple amplitudes are used to evaluate potential test liner nonlinearities (i.e., to determine the effects of source SPL on the measured impedance). More details regarding the user controls for the NIT are provided in Appendix A.

The Two-Microphone Method uses the acoustic pressures measured at the two microphone locations (2.50 and 3.75" from the liner surface) to compute the normal incidence acoustic impedance, $\zeta = \theta + i\chi$, for the liner, where θ and χ represent the normalized acoustic resistance and reactance, respectively (impedances in this paper are normalized by the characteristic impedance of air). The normal incidence absorption coefficient spectra is given by

$$\alpha(f) = \frac{4\theta(f)}{(\theta(f)+1)^2 + \chi(f)^2}. \tag{1}$$

This provides a measure of goodness for each liner, where an absorption coefficient of unity indicates complete absorption of the incoming sound at the given frequency. For a sample exposed to normal incidence sound, the optimum normalized acoustic impedance is given by $\zeta = 1.0 + 0.0\,i$. In other words, it has a real component that is unity (equal to the characteristic impedance of air) and an imaginary component that is zero. This impedance results in a perfect absorption coefficient of unity.

Test Samples

A total of 20 configurations were tested in the NIT, as listed in Table 1. A001 and A002 are representative hardwall samples constructed with aluminum and laminate, respectively. Results achieved with these two samples are used to assess the compliance of the laminate sample relative to that of the aluminum hardwall, such that this compliance can be taken into account when considering the remainder of the samples that use the laminate material.

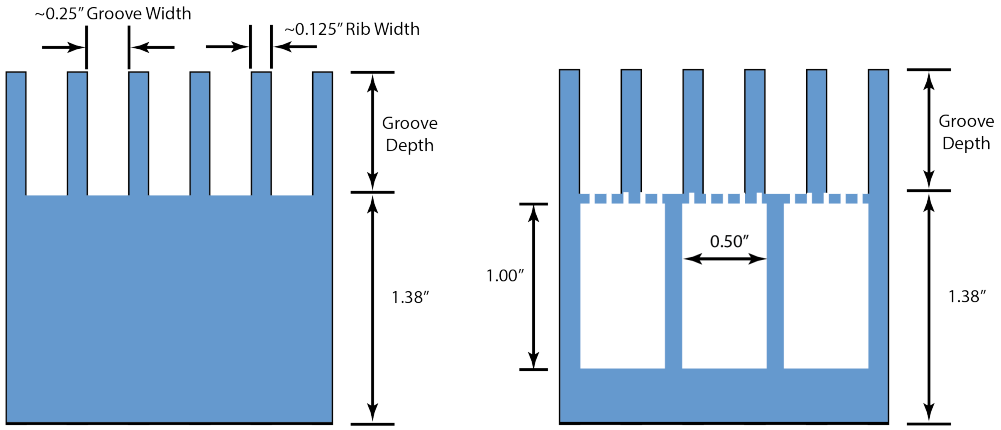
All of the remaining samples contain grooves mounted above the surface of the liner, with various groove heights. In typical aircraft applications (liners mounted in walls of an inlet or aft-bypass duct), acoustic liners do not have grooves above the surface of the liner. However, when a liner is mounted directly over the rotor, it has an impact on the aerodynamic losses related to flow around the tips of the rotors. One way to mitigate this issue is to include these grooves between the surface of the liner (above the perforate facesheet) and the rotor tips. Thus, one purpose of this study was to investigate the effects of grooves on the acoustic performance of a variety of liner configurations.

Table 1: Description of Liner Samples

Name	Description	Facesheet		Grooves
		Thickness, in	POA	Depth, in
A001	Hardwall aluminum	N/A		N/A
A002	Hardwall **laminate**	N/A		N/A
A003	Grooves with no acoustic treatment	N/A		**0.750**
A004		N/A		**0.500**
A005		N/A		**0.250**
A006	SDOF Liner with grooves	0.060	10%	**0.750**
A007		0.060	10%	**0.500**
A008		0.060	10%	**0.250**
A009		**0.030**	10%	**0.500**
A010		**0.125**	10%	0.500
A011		**0.250**	10%	0.500
A015	SDOF liner **filled with metal foam** (80 ppi, 8% density FeCrAlY), with grooves	0.060	10%	0.500
A018	Expansion chamber - **Geometry 1**	0.060	10%	0.500
A019	Expansion chamber - **Geometry 2**			
A020	Expansion chamber - **Geometry 3**			
A021	Expansion chamber - **Geometry 4**			
A022	Expansion chamber - **Geometry 5**			
A023	Expansion chamber - Geometry 5 (**no perforate**)	N/A		
A024	Expansion chamber - **Geometry 6**	0.060	10%	
A025	SDOF Liner with grooves	0.060	**20%**	0.500

Red font used to indicate parameter that changes from one sample to the next.
Core - Total depth: 1.38"; Chamber depth: 1.00"; Chamber width: 0.50"
Facesheet - Hole diameter: 0.035"
Grooves - Width: 0.25"; Rib thickness: 0.125"

Figure 4 provides an illustration of the rest of the liner configurations. Each sample consists of a 1.38"-thick core, with ribs that extend above the core to form 0.25"-wide grooves. The heights of the grooves are 0.25", 0.50", or 0.75", depending on the configuration, respectively. These configurations are clustered in four main groups.



(a) Groove-only samples. (b) SDOF samples.

Figure 4: Sketches of liner configurations.

Groove-Only Liners

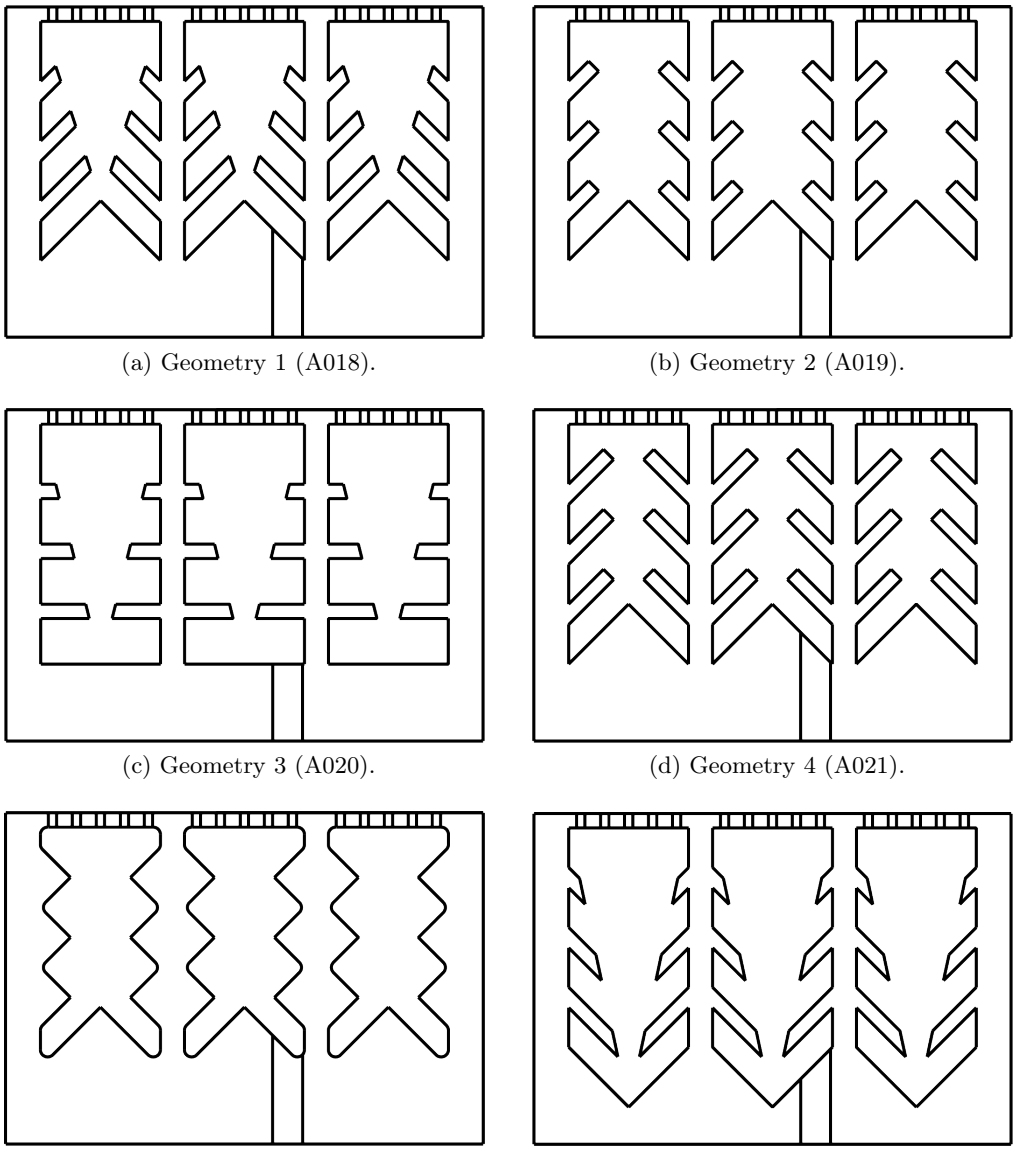
Samples A003 - A005 (Fig. 4-a; configurations A003 - A005) are used to investigate the acoustic effect of grooves for which no other absorption mechanism is included. For these liners, the only absorption mechanism is the scrubbing loss along the side walls of the ribs that form the grooves. Given the width of the grooves, this is expected to be minimal.

SDOF Liners

The next set of samples are SDOF liners (Fig. 4-b; configurations A006 - A011, A025) with chamber depths and widths of 1.00” and 0.50”, respectively. A perforate sheet is mounted above the core and below the grooves. The geometry of the perforate sheet is listed in Table 1. These samples are used to explore the effects of adding grooves (of varying depths) above conventional SDOF acoustic liners. Configuration A015 represents a slightly different version of the SDOF liner, in which the core is filled with metallic foam. This configuration is similar to those used in the original studies described earlier.

Expansion-Chamber Liners

The last set of samples (A018 - A024) replace each of the chambers of the SDOF configuration with a variety of expansion chamber geometries (Fig. 5). A023 is identical to A022, but does not include a perforate sheet between the core and the grooves. These configurations are intended to target a wider frequency range via the various expansion chamber geometries. Each of these samples had an opening in the back to allow for a temperature sensor such that the conversion of sound energy to heat could be assessed.



(a) Geometry 1 (A018).

(b) Geometry 2 (A019).

(c) Geometry 3 (A020).

(d) Geometry 4 (A021).

(e) Geometry 5 (A022).

(f) Geometry 6 (A024).

Figure 5: Expansion chamber geometries (A018 - A022, A024).

3 Results

Two sets of NIT tests were conducted for this investigation. First, results are presented for tests conducted using a broadband noise source, with the source level set to a partial overall SPL of 140 dB. These results were used to downselect among the 20 liner configurations. Five configurations were then tested using a tonal source, with source SPLs of 120, 140, and 150 dB. These results were used to more thor-

oughly evaluate each of the downselected candidate liners. For ease of comparison, all results are presented using the same frequency resolution (every 200 Hz from 400 to 3000 Hz). As the broadband results were used as a preliminary evaluation, the results presented herein are confined to absorption coefficient spectra. For the five configurations selected for more detailed study via the tonal source, both normalized acoustic impedance and absorption coefficient spectra are presented.

Broadband Results

Figure 6 presents absorption coefficient spectra for samples A001 - A005. A limited absorption coefficient scale is used due to the limited amount of absorption for these configurations. The first two samples (A001 and A002) are hardwall configurations built with different materials (aluminum and laminate). There is very little difference between the respective absorption coefficient spectra of these two configurations. Thus, at least for the purposes of the current study, the laminate material is assumed to be sufficiently rigid to have negligible effect on the overall acoustic performance of the remainder of samples (all fabricated with the same laminate material).

The other three samples (A003 - A005) are the groove-only samples with varying groove depths. As the only absorption mechanism for these samples is the scrubbing losses along the walls of the ribs, the overall poor absorption is to be expected. It is interesting to note that the shortest grooves actually provide slightly, albeit very limited, more absorption than the longer grooves. This might warrant further study in the future.

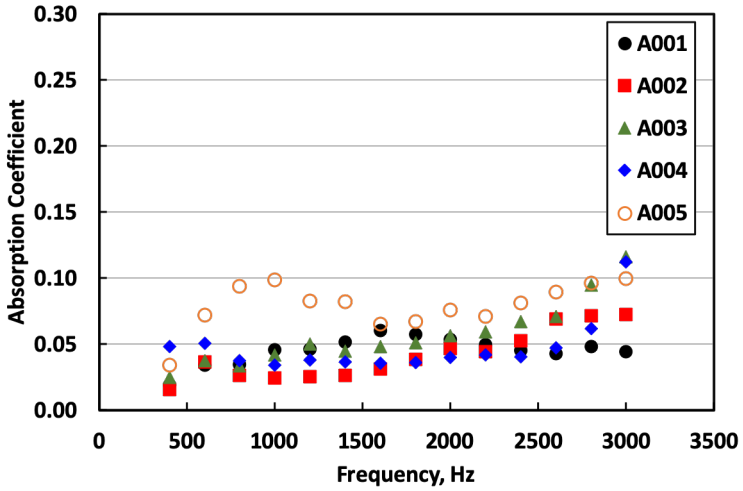


Figure 6: Absorption coefficient spectra for hardwall and groove-only samples.

Figure 7 presents the absorption coefficient spectra for samples A006 - A008, each of which has an SDOF perforate-over-honeycomb core and grooves with varying depths. The perforate facesheet for these configurations is 0.060”-thick and contains

0.035”-diameter holes, with a porosity of 10%. These simple configurations provide the expected absorption for frequencies near the quarter-wavelength resonance of the core chambers. However, the grooves clearly have an observable effect. As the depth of the grooves is reduced from 0.75” to 0.25”, the frequency of peak attenuation shifts upward, nominally by as much as 200 Hz. Regardless, the overally distribution of absorption is quite similar, indicating the groove depth is not a key factor. This offers the hope that grooves can be designed predominately for optimization of the aerodynamic performance, without having a severe deleterious effect on the acoustic performance.

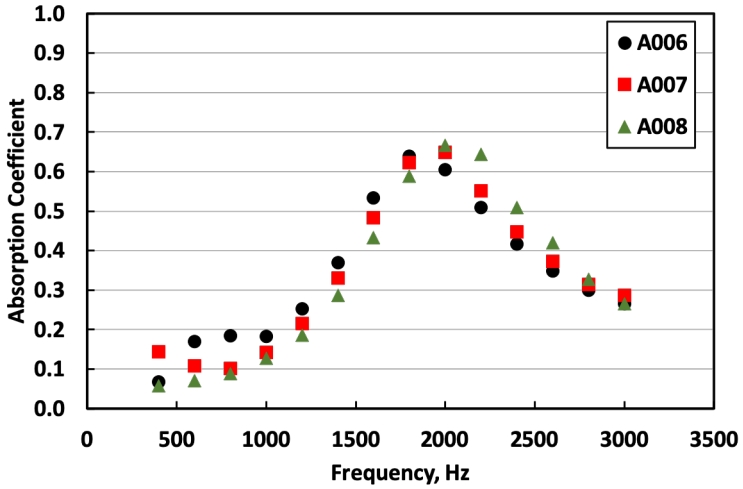


Figure 7: Absorption coefficient spectra for SDOF samples with varying groove depths.

Additional SDOF liner results are presented in Figure 8 for samples A009, A007, A010, and A011 (ordered by increasing facesheet thickness). The facesheet thickness for sample A009 is 0.030”. This thickness is roughly doubled for each successive configuration (0.030”, 0.060”, 0.125”, and 0.250”). The acoustic resistance increases as the facesheet thickness increases, and causes the absorption coefficients to also increase. It should be noted that this increase in absorption is solely due to the fact that the acoustic resistance for these samples is below the optimum for these test conditions.

The other effect of increasing the facesheet thickness is perhaps of greater importance. The mass reactance provided by the perforates increases with facesheet thickness, and correspondingly causes the resonance to shift to a lower frequency. Indeed, the frequency of peak absorption is observed to shift from approximately 2200 Hz for the 0.030”-thick facesheet to approximately 1300 Hz for the 0.125”-thick facesheet. This well-known effect is one way to tune a liner to achieve improved absorption at lower frequencies, as long as the additional mass of the thicker facesheet is acceptable.

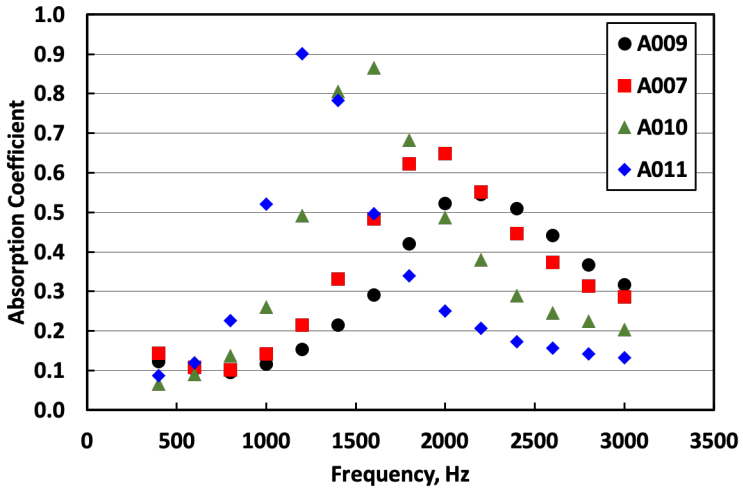


Figure 8: Effects of perforate facesheet thickness on absorption coefficient spectra for SDOF samples.

Figure 9 presents results for the A007 and A015 samples. The A007 sample is an SDOF configuration with empty core chambers, whereas the chambers are filled with metallic foam for the A015 sample. Two results are evident. First, the frequency of peak attenuation is reduced when the metallic foam is added. This is due to the decrease in sound speed through the metallic foam relative to that of air, thereby causing the chamber filled with foam to appear longer. Also, the absorption is observed to increase with the addition of metallic foam. This is due to an increase in the acoustic resistance caused by the increased tortuosity of the path through the foam-filled chamber. As noted earlier, this increase in resistance causes the absorption to increase for this particular configuration because the original configuration (empty chambers) had a resistance that was below optimum. If the facesheet had a resistance that was above optimum, the addition of metal foam would be expectd to cause the resistance to increase further above optimum, thereby causing a reduction in absorption. Regardless, use of a metallic foam filler is clearly one way to tune the liner to a lower frequency without the need for an increased liner depth.

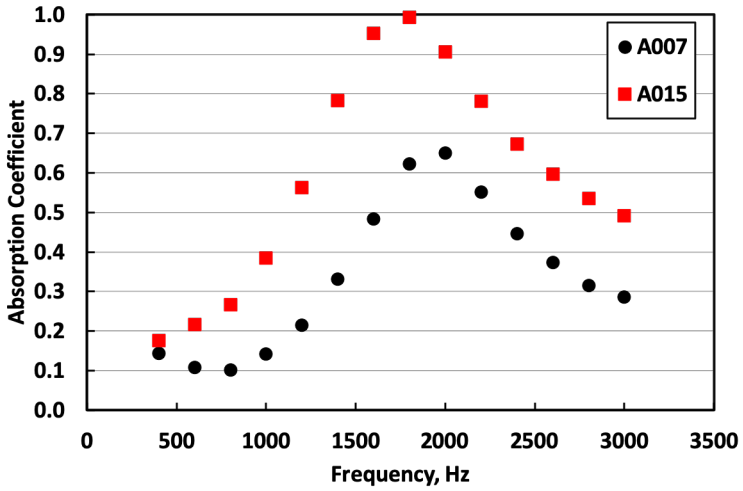


Figure 9: Effects of filling SDOF core with metallic foam.

Figure 10 presents the absorption coefficient spectra for samples A018 - A022 and A024. Each of these samples employs a different expansion-chamber configuration to replace the empty cores of the conventional SDOF liner. When compared to the results for the empty-core samples (Fig. 7), these expansion chambers provide a slight increase in absorption bandwidth. Perhaps of greater value, these results suggest that expansion chambers can provide some tuning of the absorption spectra without the need for additional liner thickness. Based on these results, the A021 configuration (Expansion Geometry 4) was selected for further analysis in other test rigs.

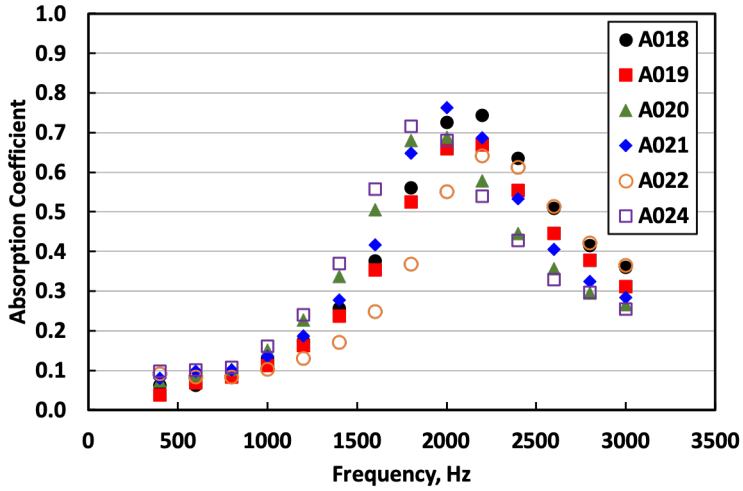


Figure 10: Effects of replacing SDOF empty cores with different expansion chambers.

Sample A018 and A023 each contain the same type (Geometry 1) of expansion-chamber cores. Whereas A018 has a perforate facesheet between the core and the grooves, A023 does not. The effects of the facesheet are readily apparent in the results of Figure 11. When the facesheet is removed, the peak absorption is shifted to a much higher frequency. As a result, the absorption in the frequency range shown in this figure is greatly reduced. Clearly, the additional resistance (for increased absorption) and mass reactance (for frequency tuning) of the perforated facesheet is needed for this application.

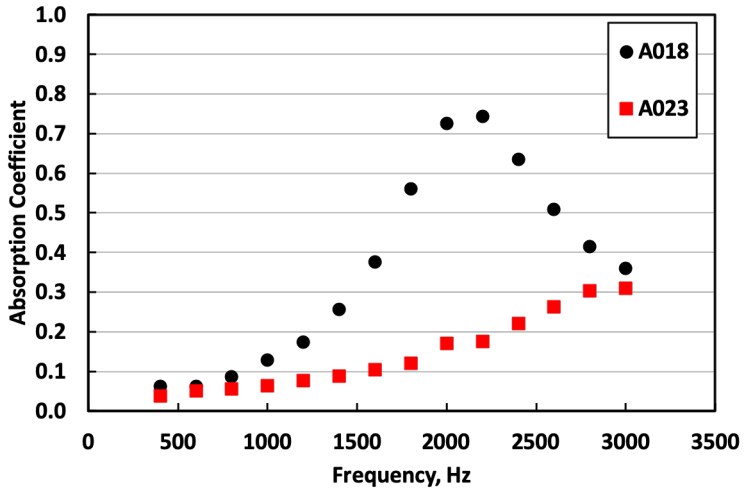


Figure 11: Effects of replacing SDOF empty cores with different expansion geometries.

Figure 12 provides a comparison of results for two SDOF samples with empty chambers. The porosity of the perforated facesheet is the only difference between these two samples. The first, A007, has a porosity of 10% (POA of 0.10) and the other, A025, has a porosity of 20%. The effects on the absorption spectra are to be expected. When the porosity increases, the resistance decreases. Recall from the earlier discussions that the original perforate (10% porosity) provides less than optimum resistance. Thus, the decrease in resistance caused by the increase in porosity results in an even lower absorption spectrum. The change in mass reactance also causes the frequency of peak absorption to shift upward by approximately 200 Hz.

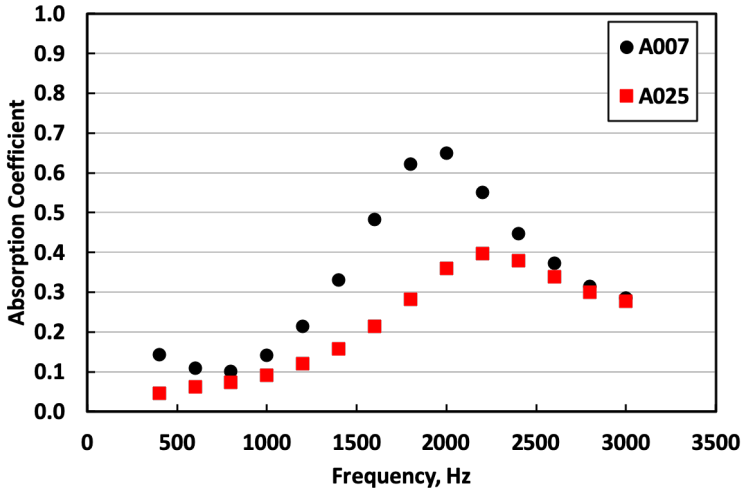


Figure 12: Effects of facesheet porosity on SDOF liner with empty cores.

Figure 13 presents a comparison of absorption coefficient spectra for two of the best configurations included in this study. The first, A015, is the SDOF configuration for which the chambers are filled with metallic foam. The second, A021, replaces the metallic foam with Expansion Geometry 4. Of these, the metallic foam liner provides improved absorption across the entire frequency range of interest. Nevertheless, both configurations perform quite well and have therefore been included in follow-on tests conducted with other test rigs.

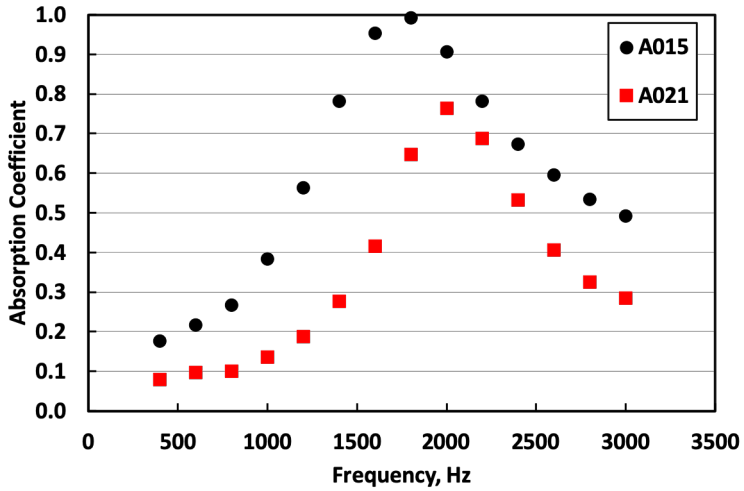


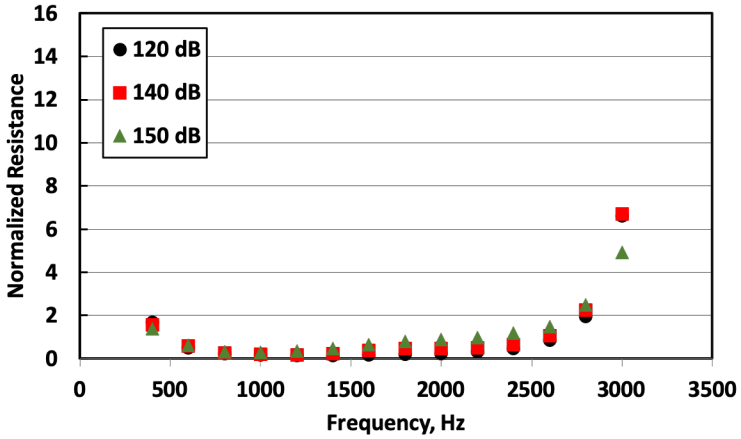
Figure 13: Comparison of optimized configurations.

Tonal Results

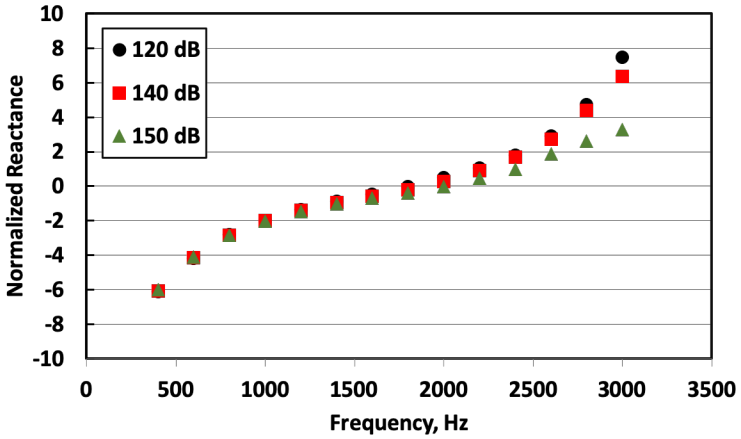
A limited number of the samples were also tested using a tonal source, to evaluate the effects of increasing the source SPL from 120 to 150 dB. The resultant normalized impedance (resistance and reactance) spectra and absorption coefficient spectra are provided in Figures 14-18.

Figures 14 and 15 present results for two SDOF liners with empty cores (conventional configuration), both with 0.500"-deep grooves but with different facesheet thicknesses (0.060" and 0.250"). As noted earlier, the increase in facesheet thickness causes the resistance to increase, especially for frequencies near resonance, and causes the resonance (frequency where the reactance transitions from a negative to positive value) to decrease by about 800 Hz. The increase in slope of the reactance spectrum for A011 indicates an increase in mass reactance, as expected. The effects of source SPL on the measured impedance are rather limited for these two configurations, with only a minor flattening of the reactance curve at the highest SPL.

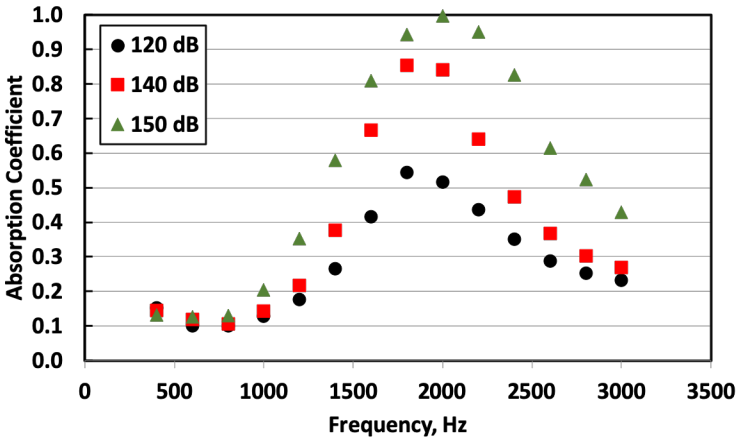
The effects of source SPL on the absorption coefficient spectra are more noticeable. Indeed, the slight differences in the impedance spectra for the sample with the thin facesheet result in significant differences in the absorption coefficient spectra. As the source SPL is increased, this sample provides increased absorption over a wider frequency range. For the sample with a thick facesheet, the results are much more subdued.



(a) Normalized resistance.

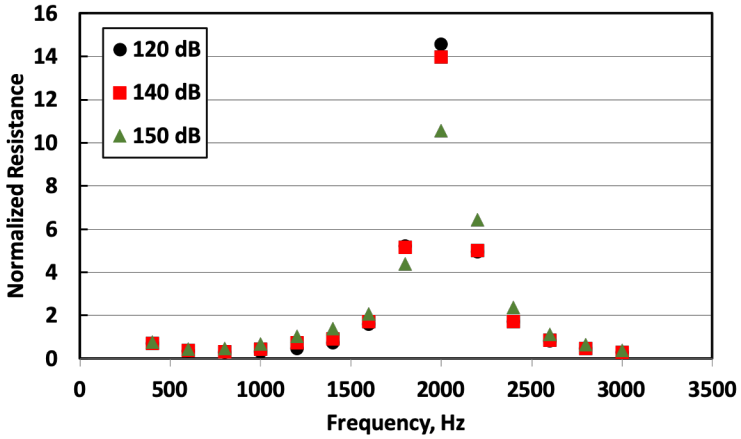


(b) Normalized reactance.

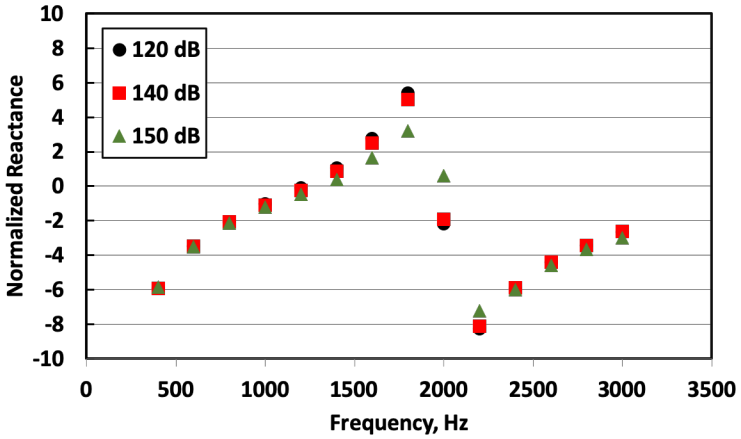


(c) Absorption coefficient.

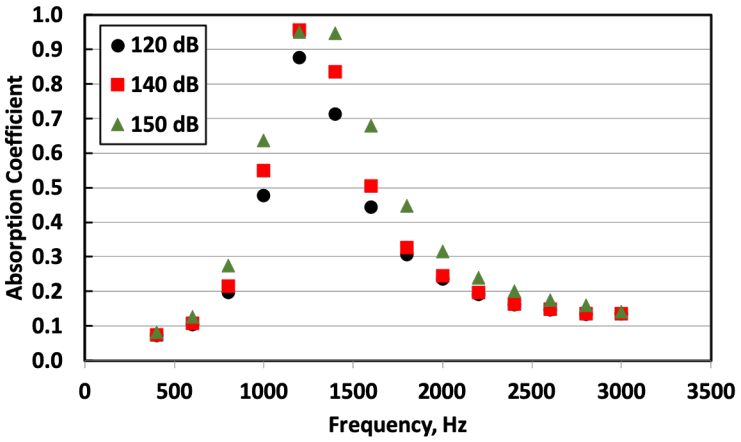
Figure 14: SDOF liner with grooves; thin facesheet (A007).



(a) Normalized resistance.



(b) Normalized reactance.

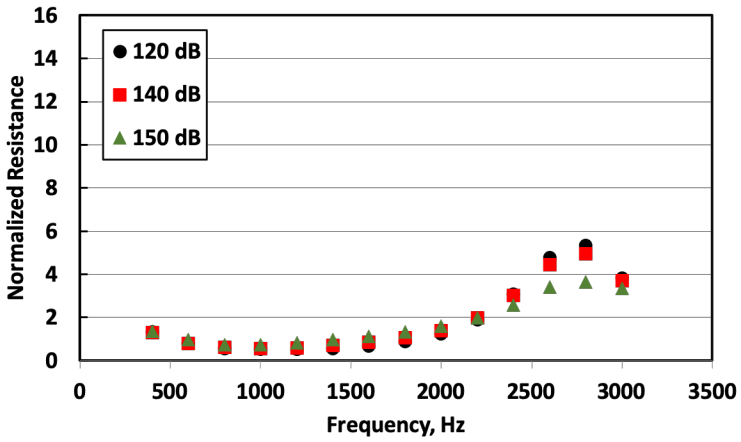


(c) Absorption coefficient.

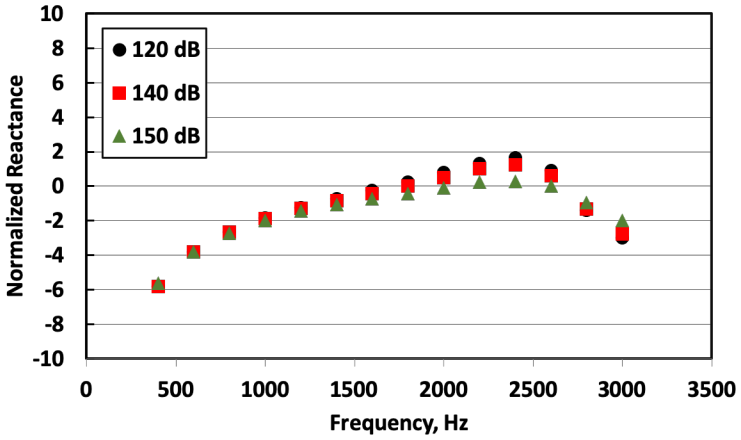
Figure 15: SDOF liner with grooves; thick facesheet (A011).

Figure 16 presents results for the the SDOF liner filled with metallic foam (A015). These tonal results are quite similar to those observed with the broadband source. The metallic foam has a strong linearizing effect on the results. Therefore, the effects of source SPL are quite limited for this sample, as expected. There is a slight increase in the range of absorption for the 150 dB case. This linearity makes this configuration very attractive, as this insensitivity to source SPL allows for more accurate predictions regarding how the liner will perform in the real (static engine or flight test) application. This is the reason this type of configuration was initially chosen for study in the early NASA over-the-rotor tests.

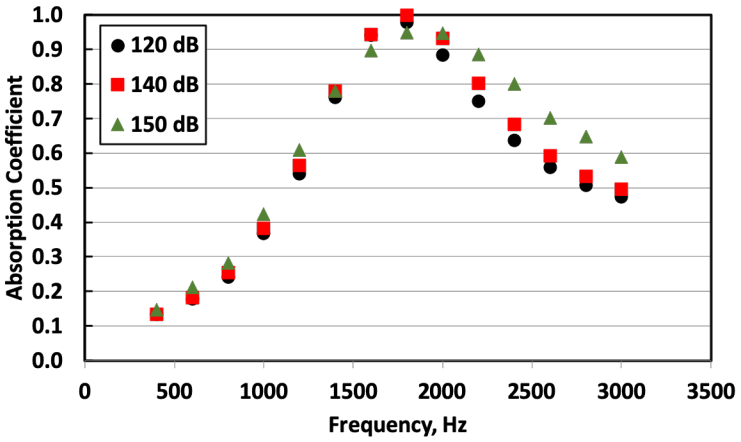
Finally, Figures 17 and 18 present tonal results for two SDOF configurations with different expansion-chamber geometries. The respective resistance spectra for the two configurations are quite similar. The corresponding reactance spectra are also quite similar, except for a very slight downward shift in resonance for A021 relative to that of A018. As noted earlier, the increase in source SPL causes the reactance spectra to flatten somewhat, especially at the highest frequencies. The resultant absorption spectra are also quite similar for the two configurations. Also, as noted earlier, slight differences in the measured impedance spectra can actually result in significant changes to the absorption spectra. As has been mentioned multiple times, the facesheet used as the baseline for this study (0.035" hole diameter, 0.060" sheet thickness, 10% porosity) provides less than the optimum amount of resistance. Thus, an increase in source SPL causes the nonlinear perforate to produce increased resistance, thereby resulting in increased absorption.



(a) Normalized resistance.

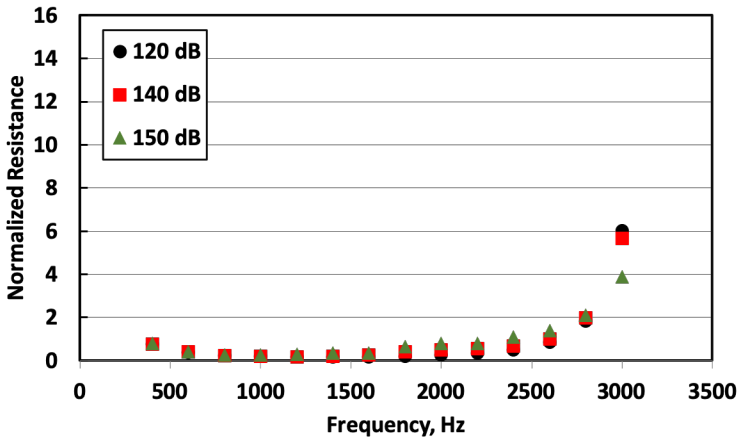


(b) Normalized reactance.

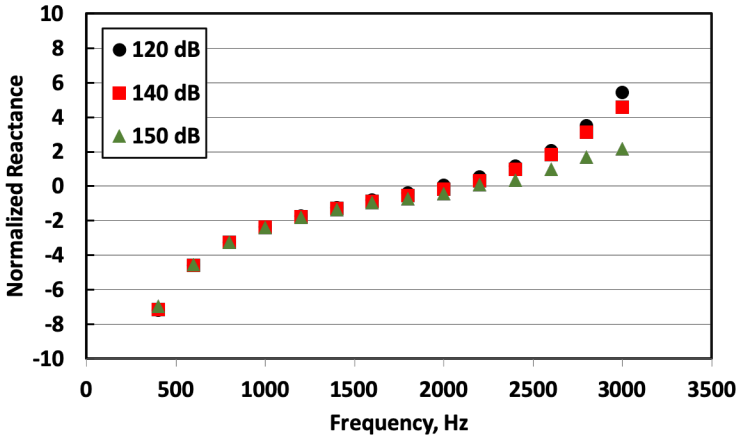


(c) Absorption coefficient.

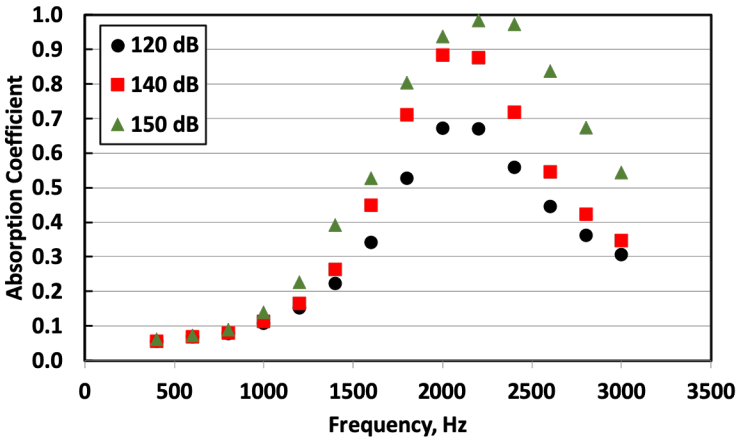
Figure 16: SDOF liner with grooves; metallic-foam filler (A015).



(a) Normalized resistance.

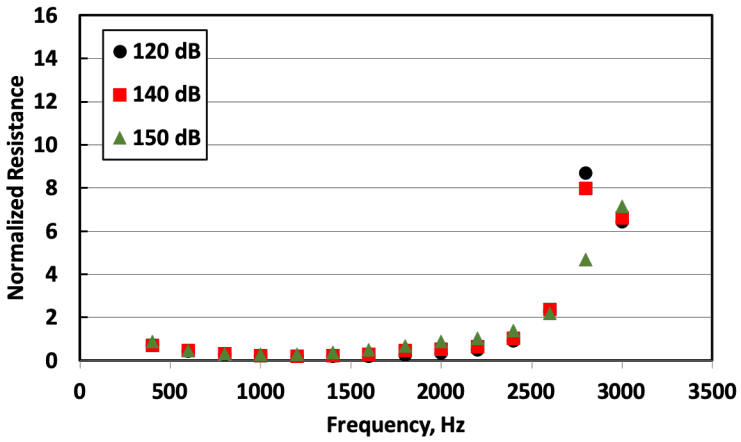


(b) Normalized reactance.

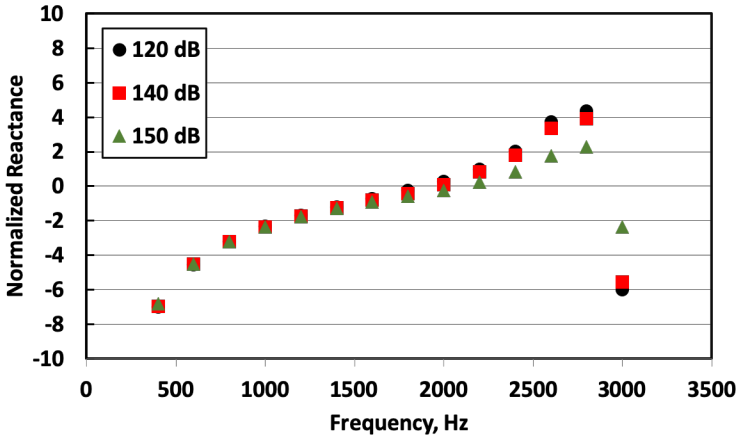


(c) Absorption coefficient.

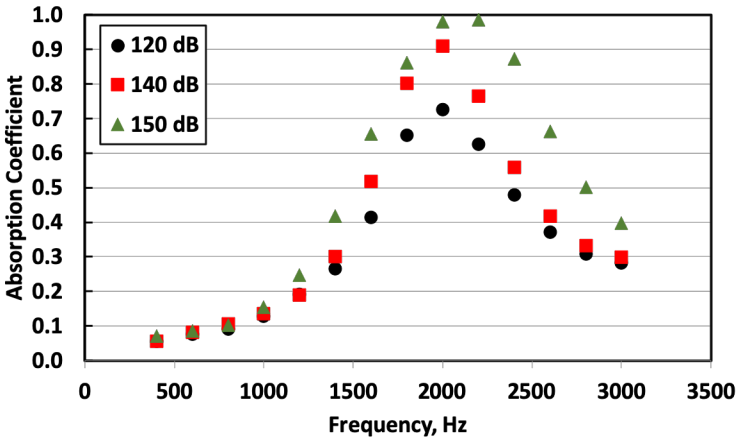
Figure 17: SDOF liner with expansion chamber core; Geometry 1 (A018).



(a) Normalized resistance.



(b) Normalized reactance.



(c) Absorption coefficient.

Figure 18: SDOF liner with expansion chamber core; Geometry 4 (A021).

4 Concluding Remarks

Results of a study of 20 acoustic liner configurations considered for use in the over-the-rotor application are presented. These results were acquired with the NASA Langley Normal Incidence Tube. The addition of grooves above the surface of the acoustic liner was demonstrated to cause minimal effect to the overall acoustic performance of these configurations. Thus, since the addition of these grooves has been separately demonstrated to be useful for reducing aerodynamic penalties caused by placing acoustic liners in the proximity of the fan rotor tips, these results suggest that they should be included in designs going forward. In general, these concepts provide the expected sound absorption.

A number of novel configurations were also included in this study. These configurations can be described as SDOF liners with the core chambers replaced by what is labeled as expansion chambers. By changing the structure of the core chambers, the resultant absorption of the liner can be slightly adjusted. The effects of perforate facesheet thickness and porosity are also demonstrated to have the expected effects, i.e., to allow for tuning of the impedance spectrum, and to shift the absorption spectrum within the frequency range of interest.

Five configurations were selected from this study for further evaluation in other test rigs. These included two conventional SDOF liners with different facesheet thicknesses, an SDOF liner filled with metallic foam, and two SDOF liners for which the core chambers were replaced with two expansion chamber geometries.

Finally, recent enhancements to the NASA Langley Normal Incidence Tube, in particular to the data acquisition routines, were presented for archival purposes.

References

1. Sutliff, D. L. and Jones, M. G., "Low-Speed Fan Noise Attenuation from a Foam-Metal Liner," *Journal of Aircraft*, Vol. 46, No. 4, July 2009, pp. 1381–1394.

2. Elliott, "Acoustic Performance of Unique Liner Locations for a High Bypass Model Turbofan at Simulated Flight Conditions," AIAA Paper 2009-3140, May 2009.

3. Jones, M. G., Parrott, T. L., Sutliff, D. L., and Hughes, C. E., "Assessment of Soft Vane and Metal Foam Engine Noise Reduction Concepts," AIAA Paper 2009-3142, May 2009.

4. Sutliff, D. L., Jones, M. G., and Hartley, T. C., "High-Speed Turbofan Noise Reduction Using Foam-Metal Liner Over-the-Rotor," *Journal of Aircraft*, Vol. 50, No. 5, September-October 2013, pp. 1491–1503.

5. Elliott, D. M., "Over the Rotor and Soft Vanes on the Source Diagnostic Test Model in the NASA Glenn 9x15 Low Speed Wind Tunnel," to be published as a NASA TM.

6. Jones, M. G. and Howerton, B. M., "Evaluation of Novel Liner Concepts for Fan and Airframe Noise Reduction," AIAA Paper 2016-2787, May 2016.

7. Gazella, M. R., Takakura, T., Sutliff, D. L., Bozak, R., and Tester, B. J., "Evaluating the Acoustic Benefits of Over-the-Rotor Acoustic Treatments Installed on Advanced Noise Control Fan," AIAA Paper 2017-3872, June 2017.

8. Bozak, R. F. and Dougherty, R. P., "Measurement of Noise Reduction from Acoustic Casing Treatments Installed Over a Subscale High Bypass Ratio Turbofan Rotor," AIAA Paper 2018-4099, June 2018.

9. Bozak, R. F., Jones, M. G., Howerton, B. M., and Brown, M. C., "Effect of Grazing Flow on Grooved Over-the-Rotor Acoustic Casing Treatments," AIAA Paper 2019-2564, May 2019.

10. Palleja-Cabre, S., Tester, B. J., Astley, R. J., and Bozak, R. F., "Modelling of Over-the-Rotor Acoustic Treatments for Improved Noise Suppression in Turbofan Engines," AIAA Paper 2017-2580, June 2017.

11. Chung, J. Y. and Blaser, D. A., "Transfer function method of measuring induct acoustic properties: I. Theory," *Journal of Acoustical Society of America*, Vol. 68, 1980, pp. 907–921.

12. Jones, M. G. and Parrott, T. L., "Evaluation of a multi-point method for determining acoustic impedance," *Journal of Mechanical Systems and Signal Processing*, Vol. 3, No. 1, 1989, pp. 15–35.

Appendix A

The NASA Langley Normal Incidence Tube (NIT) has been in operation since the mid-1970s. Numerous enhancements have been implemented over the course of that time. The purpose of this section is to provide some of the more important details regarding the current system. As noted in Section 2, the Two-Microphone Method is employed in this test rig to determine the normal incidence acoustic impedance for acoustic liner samples mounted at the termination of the duct. Sound emitted from six compression drivers impinges on and reflects from the surface of the sample. This sets up a standing wave pattern that is measured at two prescribed distances (typically 2.50" and 3.75") from the surface of the sample.

Knowledge of the test conditions (e.g., test frequency and temperatures) and these two acoustic pressures can be used to compute this standing wave pattern and, hence, the liner impedance. One key feature of the NASA NIT is the use of an automated rotating plug. This plug houses the two microphones, such that their positions can be precisely switched via an automated stepper motor. If the transfer function between the two microphone responses is measured for both configurations (i.e., first with the microphones in one orientation and then with their

orientation reversed), the 'true' differences in SPL and phase between the two microphone locations can be determined (i.e., any calibration differences between the two microphones will be canceled out).

The user typically mounts the test sample into an opening at the termination of the NIT, such that the surface is 2.50" from the first microphone in the rotating plug. If needed, it is also possible to extend the waveguide by adding inserts between the NIT termination and the test sample, such that the microphones are farther from the sample surface. This is occasionally used to allow for testing of unusual test articles that cannot fit into the opening at the NIT termination. Next, the user provides the input/output information (names of files and folders where final results are to be stored), and selects the source type (at the time of this study, either tonal or broadband), the corresponding frequency range and measurement resolution, and the target source SPL. Current tolerances are set such that the actual source SPL must be within ±0.5 dB of the target at a reference microphone mounted 0.25" from the end of the NIT. The user then presses the 'GO' button to initiate the acquisition, analysis, and storage of results.

Process control of the instrumentation is achieved by a LabVIEW-based interface (Fig. 19) executing on a computer currently running Windows 10/LabVIEW 2019. National Instruments^{TM} hardware used for measurement of signals include analog-to-digital and digital-to-analog converters, thermocouple data acquisition, and a stepper motor controller. These devices are controlled via a LabVIEW virtual instrument (VI) implemented in an asynchronous, parallel loop structure in which program functionality (and hence device control) is distributed among the loops with each loop being assigned a processing core, memory, and memory cache.

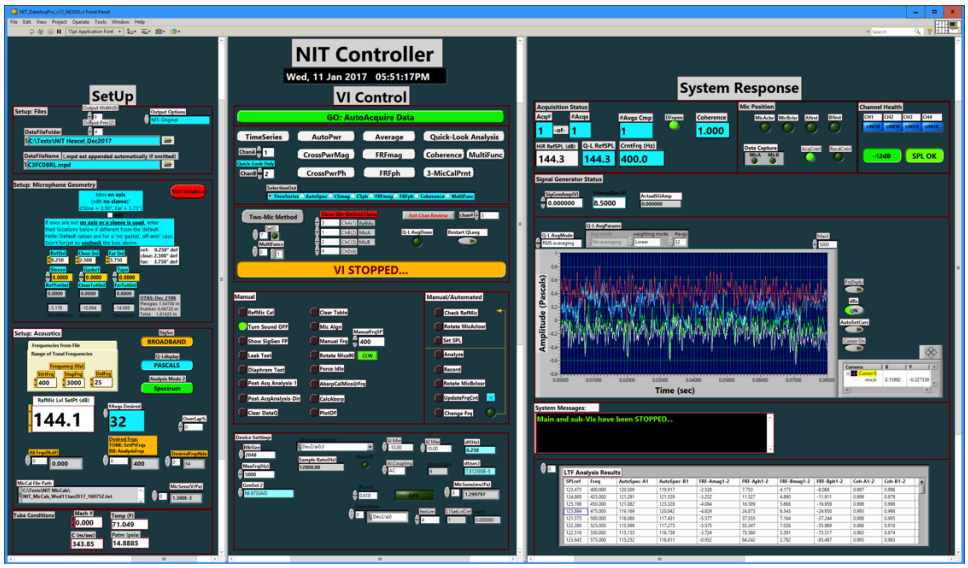


Figure 19: Main NIT front panel.

Figure 19 depicts the main NIT front panel that is initially presented to the user. Activity on the front panel is divided into Setup, VI Control, and System Response. The Setup section (see expanded view in Fig. 20) allows operator definition of data file names and output options (1.1); microphone setup geometry (1.2) such as microphone distance from sample surface, including gasket/tape thicknesses and mounting sleeve length; and acoustic analysis variables (1.3) such as measurement frequencies, reference SPL set point, and number of averages. Conditions inside the duct are also provided (1.4).

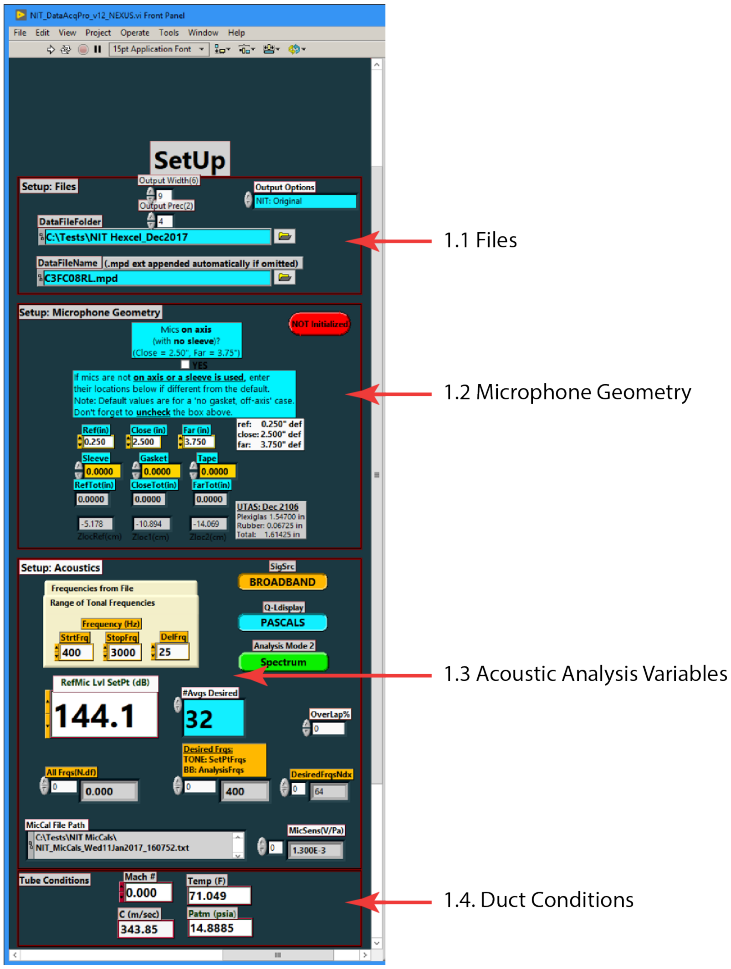


Figure 20: NIT setup section.

The Control section (Fig. 21) provides a combination of automated and manual acquisition and analysis options for production and nonstandard (i.e., exploratory) research data sets. The large green "GO" button (2.1) at the top initiates production–style automated system execution, including acquisition, analysis, and storage of results, based upon the discrete frequencies and SPL set point of interest defined in

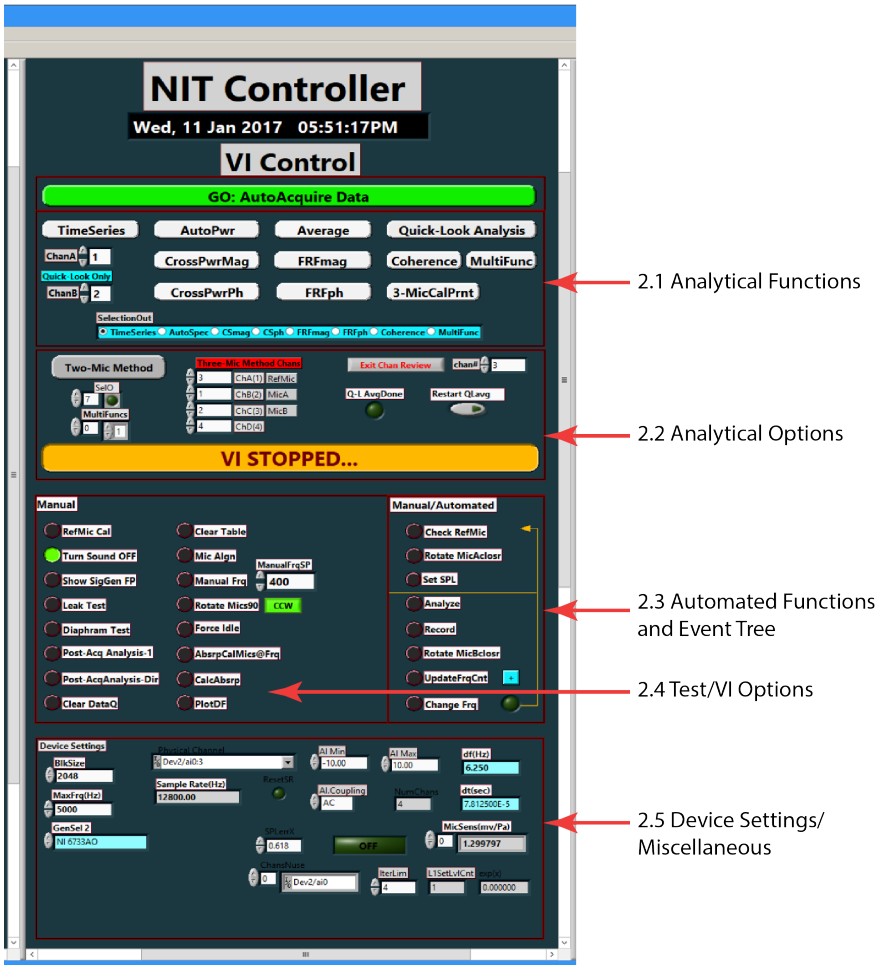


Figure 21: NIT controller section.

the Setup Section. Each element on the Manual/Automated event tree (2.3 in the center right of the panel) is illuminated while that portion of activity is in progress. Conversely, the operator can choose to perform these activities for nonstandard analysis by pushing each button as desired. A variety of signal processing analyses (2.1) ranging from auto/cross power spectra to frequency response to coherence to multiple functions with one click, and options for analysis methods are also available (2.2). Some of the more important functions (2.4) include vertical alignment of the microphone plug, post-acquisition data analysis, microphone calibration control, and analog speaker voltage generator. System device settings and miscellaneous controls pertinent to setting SPL level (2.5).

The System Response section (Fig. 22) displays current run-time information such as acquisition status, microphone position, data channel health, plotted and tabularized selected analytical results, and system messages. The acquisition status

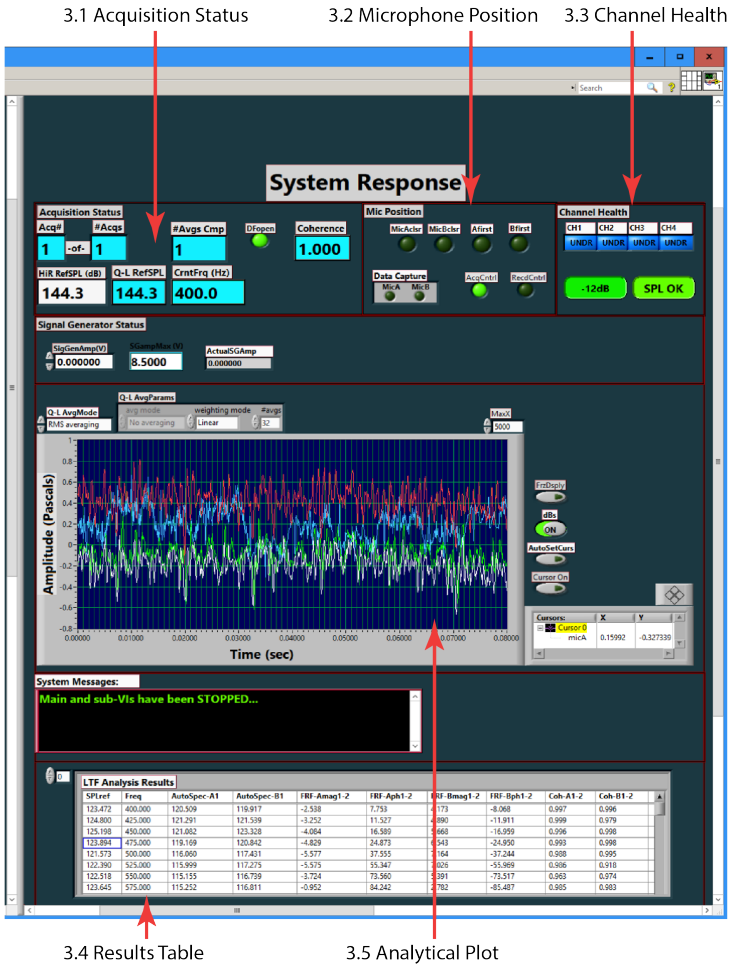


Figure 22: NIT system response section.

(3.1) indicates the current data point being taken, the maximum SPL and associated frequency, and coherence. The microphone position (3.2) is also provided relative to the sample and data collection order. Channel health (3.3) is provided in terms of signal strength relative to the reference microphone, and also if the reference microphone is within ± 0.5 dB of the SPL set point. A tabulated spreadsheet of each acquisition analytical results is presented (3.4), and graphical depiction of the spectral data are also shown (3.5).

REPORT DOCUMENTATION PAGE

Form Approved
OMB No. 0704–0188

The public reporting burden for this collection of information is estimated to average 1 hour per response, including the time for reviewing instructions, searching existing data sources, gathering and maintaining the data needed, and completing and reviewing the collection of information. Send comments regarding this burden estimate or any other aspect of this collection of information, including suggestions for reducing this burden, to Department of Defense, Washington Headquarters Services, Directorate for Information Operations and Reports (0704-0188), 1215 Jefferson Davis Highway, Suite 1204, Arlington, VA 22202-4302. Respondents should be aware that notwithstanding any other provision of law, no person shall be subject to any penalty for failing to comply with a collection of information if it does not display a currently valid OMB control number.
PLEASE DO NOT RETURN YOUR FORM TO THE ABOVE ADDRESS.

1. REPORT DATE *(DD-MM-YYYY)*	2. REPORT TYPE	3. DATES COVERED *(From - To)*
01-12-2019	Technical Memorandum	

4. TITLE AND SUBTITLE
Over-the-Rotor Liner Investigation via the NASA Langley Normal Incidence Tube

5a. CONTRACT NUMBER

5b. GRANT NUMBER

5c. PROGRAM ELEMENT NUMBER

6. AUTHOR(S)
Michael G. Jones, Martha C. Brown, Brian M. Howerton, Lawrence E. Becker

5d. PROJECT NUMBER

5e. TASK NUMBER

5f. WORK UNIT NUMBER
081876.02.07.12.01.02

7. PERFORMING ORGANIZATION NAME(S) AND ADDRESS(ES)
NASA Langley Research Center
Hampton, Virginia 23681-2199

8. PERFORMING ORGANIZATION REPORT NUMBER
L–21083

9. SPONSORING/MONITORING AGENCY NAME(S) AND ADDRESS(ES)
National Aeronautics and Space Administration
Washington, DC 20546-0001

10. SPONSOR/MONITOR'S ACRONYM(S)
NASA

11. SPONSOR/MONITOR'S REPORT NUMBER(S)
NASA/TM–2019–220430

12. DISTRIBUTION/AVAILABILITY STATEMENT
Unclassified-Unlimited
Subject Category 71
Availability: NASA STI Program (757) 864-9658

13. SUPPLEMENTARY NOTES

14. ABSTRACT
NASA Langley and Glenn Research Centers have collaborated on the usage of acoustic liners mounted very near or directly over the rotor of turbofan aircraft engines. This collaboration began over a decade ago with the investigation of a metallic foam liner. Similar to conventional acoustic liner applications, this liner was designed to absorb sound generated by the rotor-alone and rotor-stator interaction sources within the fan duct. Given its proximity to the rotor tips, the expectation was that the liner would also serve as a pressure release and thereby inhibit the amount of noise generated. Initial acoustic results were promising, but there was concern regarding potential aerodynamic penalties. Nevertheless, there were sufficient positive results to warrant further investigation. To that end, the current report presents results obtained in the NASA Langley Normal Incidence Tube for 20 acoustic liner candidates for the OTR application. The majority contain grooves at their surface, designed to minimize aerodynamic penalties caused by placing the liner in close proximity to the fan rotor tips. The intent is to assess the acoustic properties of each liner configuration, and in particular to assess the effects of including the grooves on the overall acoustic performance. An additional intent of this paper is to provide documentation regarding recent enhancements to the NASA Langley Normal Incidence Tube.

15. SUBJECT TERMS
liner, flow resistance, duct acoustics, normal incidence tube

16. SECURITY CLASSIFICATION OF:			17. LIMITATION OF ABSTRACT	18. NUMBER OF PAGES	19a. NAME OF RESPONSIBLE PERSON
a. REPORT	b. ABSTRACT	c. THIS PAGE			STI Information Desk (help@sti.nasa.gov)
U	U	U	UU	15	19b. TELEPHONE NUMBER *(Include area code)* (757) 864-9658